Influence of process parameters on the adsorption properties of zeolite 13X

Ognjen Stojkić[1], Radislav Filipović[1,2], Mladen Janković[2], Mitar Perušić[1], Duško Kostić[1,3], Srećko Stopić[3], Vladimir Damjanović[2]*

[1]*Faculty of Technology, University of East Sarajevo, Zvornik, Republic of Srpska, Bosnia and Herzegovina*
[2]*Alumina Ltd., Zvornik, Republic of Srpska, Bosnia and Herzegovina*
[3]*IME Process Metallurgy and Metal Recycling, RWTH Aachen University, Aachen, Germany*

ISSN 2712-1267
UDC: 549.67:577.164.1
https://doi.org/10.59919/JCTE05202401005
Original scientific paper

Paper received: 12 Nov 2024
Paper accepted: 17 Dec 2024
Paper available from 31 Dec 2024
at https://glasnik.tf.unibl.org/

Keywords:
adsorption, characterization, process parameters, zeolite.

Zeolite 13X is one of the best adsorbents among zeolites and one of the most commercially available zeolites. The field of application of this material continues to expand, as does the market, but at the same time, stricter requirements are being set for the quality of this product in terms of phase purity, adsorption characteristics, and stability in different application conditions. The company Alumina Ltd. Zvornik has recently been producing 13X zeolite, but the desire to win a larger market share and more economical production requires further research work on the synthesis of this material. Therefore, the subject of this paper is the investigation of the influence of several process parameters on the properties of 13X zeolite, including crystallization temperature, crystallization duration and Si/Al molar ratio in the starting reaction mixture. The quality of the obtained powders was examined in detail through a series of analytical and instrumental methods, the results of which are presented in the paper. Water and CO_2 adsorption capacities were determined as key quality parameters of 13X zeolite, and additional characterization was performed by determining material granulometry, specific surface area (BET analysis), crystallinity (X-ray diffraction method) as well and SEM analysis. The obtained results indicate a clear dependence between the examined process parameters of the system and the characteristics of the synthesized materials, thus enabling the selection of optimal conditions for the synthesis of 13X zeolite.

INTRODUCTION

Zeolites are nanoporous crystalline materials consisting of SiO_4 and AlO_4 tetrahedra, connected through shared oxygen atoms (Auerbach et al., 2003; Garshasbi et al., 2017). In general, the chemical composition of zeolites can be represented by the formula $M_{x/n}[(Al_2O_3)_x \bullet (SiO_2)_y)] \bullet mH_2O$, where the negatively charged aluminosilicate skeleton is neutralized with an M cation of valence n, m is the number of water molecules per unit cell, and x and y are the total numbers of tetrahedra per cell (Auerbach et al., 2003; Tahraoui et al., 2020). The way the zeolite crystal lattice is built provides the possibility of forming a large number of different types of crystal forms, and more than 250 structures are known today, of which about 40 are present in nature, while the other types are synthesized (Database of Zeolite Structures, n.d.). However, only a few crystalline types of zeolites find significant commercial applications, where under the same structural type we can distinguish materials based on the chemical composition of the crystal lattice, the type of bound cation, etc. Different types of zeolites within the same structural type are mostly created synthetically, where based on a series of synthesis parameters, the system is managed towards the creation of products with certain characteristics, depending on the planned use of the material. Zeolites are mainly synthesized in hydrothermal conditions (Garshasbi et al., 2017), that is, from aqueous solutions of the starting components under conditions of elevated temperature and elevated steam pressure in the system.

One of the most commercially available zeolites is 13X zeolite (Collins et al., 2020; Janković et al., 2023; Price et al., 2017). As raw materials for zeolite synthesis are typically a sodium aluminate ($NaAlO_2$) solution, serving as the source of sodium (Na) and aluminum (Al), and waterglass, which provides the source of silicon (Si), sodium hydroxide (NaOH) for pH control and dissolution of raw materials and distilled water for dilution and homogenization of the mixture (Janković et al., 2023; Liu et al., 2024).

This is a synthetic zeolite that copies the crystal lattice form of the natural zeolite mineral Faujasite, and this type of zeolite crystal structure is designated as FAU. Thanks to the characteristics of this crystal structure, which has cavities (pores, cage) with the largest volume among zeolites and its composition, which

**Corresponding author:*
Duško Kostić, IME Process Metallurgy and Metal Recycling, RWTH Aachen University, Aachen, Germany;
email: dkostic@metallurgie.rwth-aachen.de

implies a low molar ratio of Si/Al and a large number of compensating cations, 13X zeolite stands out primarily for its adsorption and separation capabilities and expresses also catalytic possibilities. Based on that, this material is used in a large number of industrial processes where the mentioned properties are important (Chen et al., 2018; L. Liu et al., 2012; L. Y. Liu et al., 2014). Among those processes, some of the most important are the production of oxygen (Al-Shawabkeh et al., 2023; Gholipour & Mofarahi, 2009; Houchins et al., 2020; Mofarahi & Shokroo, 2013; Shirani et al., 2010), the processing of natural gas and liquid petroleum gas (Brea et al., 2019; Esfandian & Garshasbi, 2020; Gholipour & Mofarahi, 2009), industrial production and purification of hydrogen (Brea et al., 2019; Zafanelli et al., 2024), production and refining of biofuels (Alshahidy & Abbas, 2021; Bareschino et al., 2020; Shirani et al., 2010), industrial production and purification of alcohol (Sigot et al., 2016), refining of petroleum compounds (Esfandian & Garshasbi, 2020; Sigot et al., 2016) and so on. Much of the use of 13X zeolite is based on its hydrophilicity and high water adsorption capacity. In addition to the above, the high adsorption capacity of CO_2 and other gases that cause the "greenhouse" effect have recently added importance and expanded the possibilities of using 13X zeolite (Al-Shawabkeh et al., 2023; Anbia et al., 2015; Chen et al., 2018; Cmarik & Knox, 2018; Morales-Ospino et al., 2020; Shirani et al., 2010; Yahya & Hussein, 2019). Due to the aforementioned properties, increasingly strict requirements for product quality, as well the potential growth of needs due to the development of new adsorption processes, especially those processes related to the reduction of "greenhouse" gas emissions, it is of great importance to find optimal parameters for the synthesis of this type of zeolite for wider commercial use (Janković et al., 2023).

Considering the large number of different types of zeolites, and similar synthesis conditions where very often a difference in temperature or concentration of a few percent can alter the formation of different types of zeolites, it is necessary to define all the process parameters that affect the synthesis and precisely determine their values that will result in the synthesis of the appropriate material and its satisfactory characteristics. Accordingly, the subject of this paper is the investigation of the influence of several very important process parameters on the quality of synthesized 13X zeolite powders and the determination of the optimal values of these parameters for synthesis.

MATERIALS AND METHODS

Experimental syntheses of zeolite 13X were performed in the laboratory of Alumina Ltd. in Zvornik, as part of a wider research work on determining the technological parameters for the production of this zeolite. The used laboratory reactor has a volume of 1l, equipped with a vertical mixer and a system for indirect heating and maintaining the set temperature of the suspension in the reactor.

The starting raw materials for the synthesis were:

- Water glass (aqueous solution of sodium silicate, Na_2SiO_3) obtained by dissolving quartz sand (SiO_2) in NaOH solution, which is produced at the Alumina Ltd. factory for the production of zeolite and silica gel;
- Sodium aluminate solution ($NaAlO_2$) obtained by dissolving aluminium hydrate ($Al(OH)_3$), approximate Al_2O_3 content of 65%) in NaOH solution;
- NaOH solution (50%) purchased for industrial use in the factory (BorsodChem, Hungary);

The syntheses were performed in such a way that the calculated amount of water and water glass were first dosed into the reactor. The required amount of NaOH solution was used to dissolve aluminium hydrate, and the resulting sodium aluminate was then, with mixing, dosed into the reactor containing the water glass solution. After preparing the reaction mixture, it was homogenized by mixing for 60 minutes at room temperature and then heated to the set crystallization temperature. The mixture was stirred at a constant speed all the time.

A total of 10 syntheses were performed, and the experiment was designed so that four syntheses can be used in three series, i.e. to demonstrate the influence of three important process parameters, namely crystallization temperature, crystallization time and the Si/Al molar ratio of the starting reaction mixture. Other process parameters were of equal and constant values in all syntheses. Table 1 shows the values of the examined process parameters for all syntheses. The marked values were changed in the corresponding series of samples. In addition, in Table 1 also lists the alkalinity indicator of the synthesis system, expressed through the concentration of Na_2O in the basic solution after the synthesis reaction. This parameter shows an approximately constant value for all tested samples.

Chemical analysis of the zeolite composition and content determination was performed on a Shimadzu AA-7000 atomic adsorption spectrophotometer.

Water adsorption capacity (WAC) was tested using a Cambic KK-105-CH air chamber (CiK Solutions GmbH, Germany) in conditions that included a temperature of 20°C and relative humidity of rH=50±2, during 24 hours. Thermal activation was performed at a temperature of 350 to 550°C.

Table 1. Process parameters for the 10 shown experimental syntheses

Sample	1	2	3	4	5	6	7	8	9	10
Crystallization temperature, $T_{cr.}$ [°C]	82	86	90	94	90	90	90	90	90	90
Crystallization time, $\tau_{cr.}$ [*min*]	330	330	330	330	210	270	390	330	330	330
Molar ratio Si/Al starting mixture, M [-]	1,35	1,35	1,35	1,35	1,35	1,35	1,35	1,40	1,30	1,25
Concentration Na_2O, $C_{(Na_2O)\ M.R.}$ [*g/l*]	54,14	56,41	56,25	55,17	55,89	54,08	53,62	56,71	56,02	53,98

The determination of the specific surface area of the synthesized samples was carried out according to the BET method (abbr. from Brunauer–Emmett–Teller) in a stream of gaseous nitrogen (N_2) on a GEMINI VII device (Micromeritics Instrument Corporation, USA) with the preparation of a 13X zeolite sample by thermal activation for 4 hours at 520° *C* and 1h at 400°C and degassing in a stream of nitrogen in the corresponding Flow-Prep block.

The CO_2 adsorption capacity was also determined by analysis on the same device as the BET method, with sample preparation by degassing for 4 hours at 520°C and 1 hour at 400°C.

Recording of the diffractogram and determination of the degree of relative crystallinity was performed on a Bruker D8 ENDEAVOR diffractometer with an X-ray tube with a cobalt anode, i.e. using CoKα radiation with a wavelength of λ=1.78897Å, in the range of diffraction angles 2Θ from 25.0 to 29.0°, with an angle change step of 0.02° and an exposure of 0.50s per step. The internal standard sample of the laboratory at Alumina Ltd. was used to determine the crystallinity by comparison method.

Imaging of zeolite crystals with a scanning electron microscope was performed in the laboratory of the Faculty of Technology and Metallurgy in Belgrade using the MIRA3 TESCAN device (TESCAN Group a.s., Czech Republic), with magnifications of up to 10,000 times at 20kV. Prior to analysis, all samples were prepared by spraying a layer of gold using a sprayer to avoid the build-up of an electrostatic charge.

Determination of mean diameter (D_{50}) and particle size distribution was performed on a CILAS 1090 liquid device (CPS, USA) in the range from 0.02 to 500 μm, with 30 seconds of ultrasonic sonication

RESULTS AND DISCUSSION

Effect of crystallization temperature

Syntheses performed in reaction systems at different temperatures showed a great dependence on the properties of the obtained powders. The results of the sample analysis are listed in Table 2, and the basic derived dependencies are shown in Fig. 1 and Fig. 2.

Table 2. Results of analysis of 13X zeolite powders synthesized at different crystallization temperatures

Synthesis number	Tcr. [°C]	D50 [*μm*]	Si/Al ratio [-]
1	82	4,03	1,120
2	86	3,82	1,090
3	90	3,40	1,135
4	94	3,55	1,135

As can be seen, the change in the crystallization temperature significantly affects the crystallinity of the synthesized powders (Fig. 1). According to this dependence, the influence is expressed on other determined characteristics of the material. Increasing the crystallization temperature from 82 to 94°C led to a drastic increase in the relative crystallinity of the material (Fig.1).

The high crystallinity of 13X zeolite synthesized at higher temperatures indicates that these powders are also of high purity crystalline phase, that is, there is no significant presence of other crystalline structures or amorphous phase. Thanks to this, the desired characteristics of 13X zeolite are expressed in the samples obtained at higher temperatures, which distinguish this material from other similar materials - first of all, a large specific surface area (Fig. 1) which further contributes to good adsorption properties, i.e. a high adsorption capacity of water and carbon dioxide (CO_2). The values of these parameters constantly increase with increasing crystallization temperature (Fig. 2).

Figure 3 shows the comparative results of the XRD analysis of the samples synthesized at different crystallization temperatures, which confirm the aforementioned observations. The diffractograms of the samples from syntheses 1 and 2, performed at lower temperatures, have well-defined characteristic peaks of 13X zeolite without the presence of an

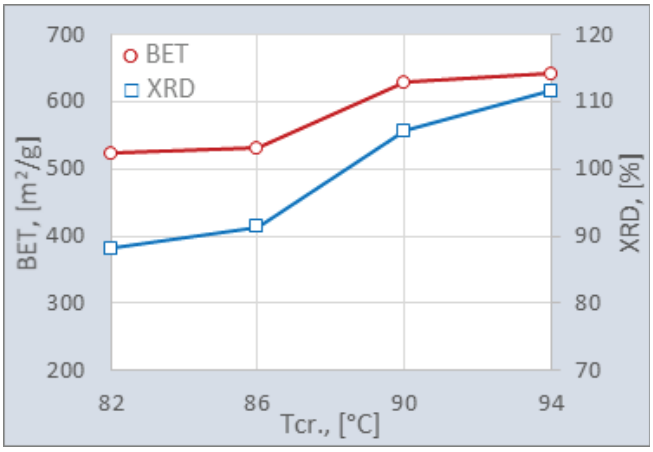

Figure 1. The trend of crystallinity (□) and specific surface (○) values of the material in relation to crystallization temperature

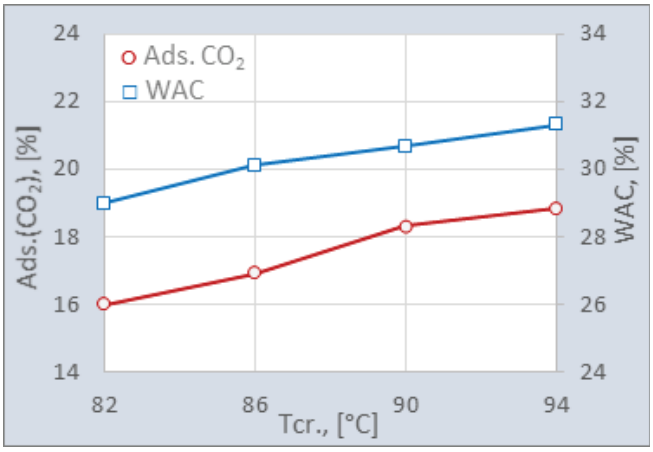

Figure 2. Trend of water adsorption (□) and carbon dioxide adsorption (○) values in relation to crystallization temperature

amorphous phase, which corresponds to the observed values of the results of the analyses of these samples, which have a relative crystallinity close to 90% and receptive values of the specific surface area and H_2O and CO_2 adsorption capacity. However, it is noticeable that the intensity of the characteristic peaks in these samples are much lower than the samples obtained at higher temperatures, which corresponds to the difference in crystallinity. In addition, the diffractograms of the samples synthesized at lower temperatures, 82 and 86°C, show the significant presence of another crystalline phase, namely 4A (LTA) zeolite, which corresponds to the fact that this type of zeolite is synthesized under conditions similar to the synthesis of 13X zeolite, but mostly at a lower temperature and the Si/Al molar ratio. The presence of the 4A crystalline form is highest in the sample from synthesis 1 obtained at 82°C. Zeolite 4A type, although also a commercially very common material and valued for its adsorption characteristics and the selectivity of its crystal lattice towards molecules of a certain size, has a lower specific surface area and worse adsorption characteristics than 13X zeolite. Because of this, and since it can prevent the diffusion and adsorption of certain molecules on 13X zeolite, the observed presence of this phase in 13X zeolite samples is considered an impurity and reduces the quality of the synthesized powders, which is shown by the above results.

On the other hand, the diffractograms of the samples synthesized at higher temperatures show a pure and highly crystalline phase of 13X zeolite, which certainly corresponds to the very good results of the analysis of these samples. The calculated crystallinity values of these two samples, based on the comparison with the standard sample, showed extremely high values, even higher than the standard sample. Figure 4 shows the results of the comparative XRD analysis of the sample from synthesis 4 (T_{cr}.=94°C) and the standard sample of 13X zeolite, where it can be seen that the peak intensities of S4 powder are significantly higher, which

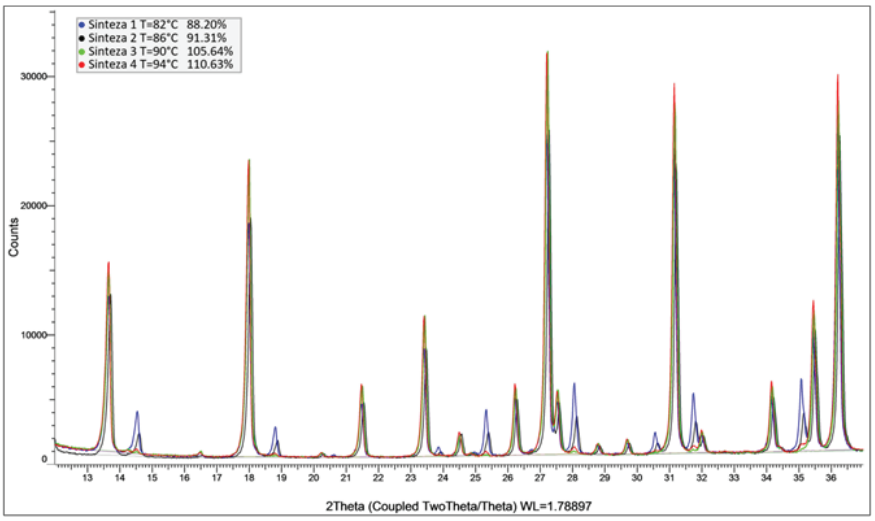

Figure 3. Diffractogram for samples of syntheses 1-4, performed at different crystallization temperatures

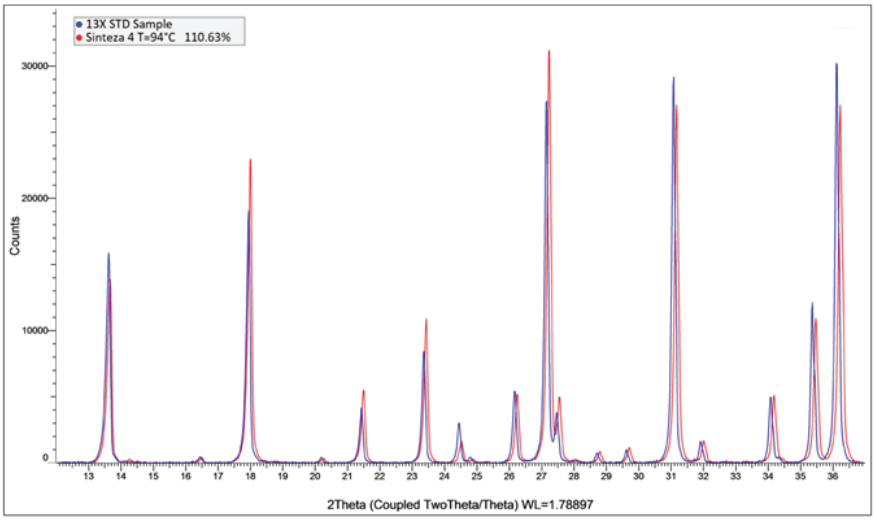

Figure 4. Diffractogram for sample 4, performed at Tcr.=94°C, in relation to the standard sample of 13X zeolite

led to a higher value of crystallinity. In addition, it can be seen that there is practically no other crystalline phase that deviates from the standard diffractogram, which confirms the high purity of the crystalline phase of this material.

Based on Table 1 it can be seen that the Si/Al molar ratio is significantly lower in the synthesized powders than it was in the initial reaction mixture. A greater presence (so-called "excess") of silicon in the initial mixture causes a greater residue of this species in the mother solution after the crystallization reaction, and its share in the crystalline phase decreases accordingly, which also reduces the ratio of Si/Al atoms. The Si/Al ratio in the samples from syntheses 1 and 2 is nevertheless visibly lower than in samples 3 and 4, which corresponds to the significant presence of the 4A phase in the first two syntheses, as 4A zeolite during crystallization generally tends to the composition with the lowest possible Si/Al ratio of approx. 1.

SEM images of samples from the first four syntheses are shown in Figure 5. The powders in all images shown are characterized by well-defined crystallites of relatively uniform size and shape. This corresponds to the results of XRD analysis, i.e. samples of high relative crystallinity without significant presence of amorphous phase even at the lowest crystallization temperature.

It can be said that with the samples synthesized at lower temperatures and with the 4A zeolite phase present, there is a tendency towards the formation of smaller agglomerates by joining crystallites. This corresponds to a slightly larger value of the measured average particle diameter of these samples (Tab. 1). On the other hand, an increase in the crystallization temperature should favour the growth of crystallites, however, their connection into smaller agglomerates

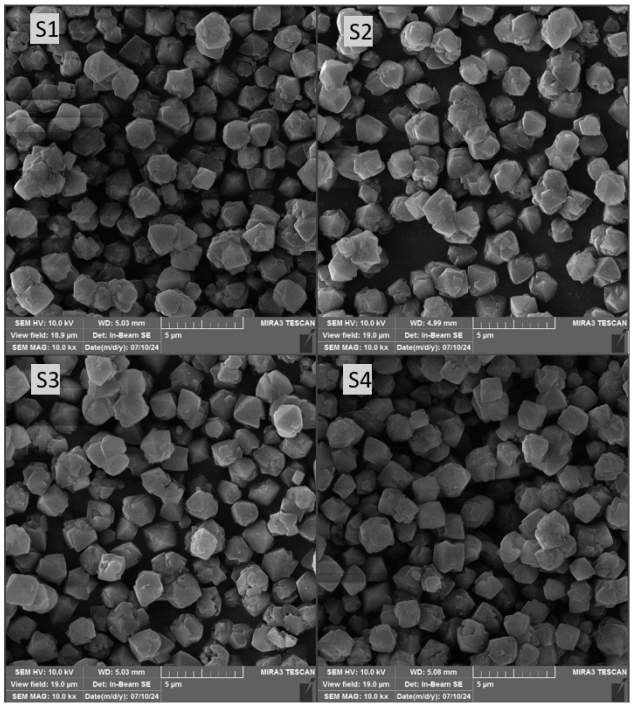

Figure 5. SEM images of samples from syntheses 1-4, performed at different crystallization temperatures

in samples 1 and 2 still has the effect of compensating for the effect of a slightly higher crystallization temperature and leads to a larger average particle diameter of these samples. In general, the observed difference in mean diameter values is not large.

Effect of crystallization time

The syntheses performed during different crystallization reaction times helped to determine the optimal duration of the synthesis and a better understanding of the changes in the reaction system during the synthesis. The results of the analysis of the samples from these syntheses are listed in Table 3,

and the basic derived dependencies are shown in Fig. 6 and Fig. 7. Due to the wide range of investigated crystallization times, the influence of this parameter on the crystallinity of 13X zeolite and other properties of the obtained powders is clearly expressed. Similar to the previous part, the changes in the value of the specific surface area of the material as well as the change in the adsorption capacity of water and carbon dioxide almost completely follow the trend of the change in the crystallinity of the material (Fig. 1 and Fig. 2).

The shortest applied crystallization time is not enough to obtain a material with relevant characteristics. The low degree of crystallinity of the material indicates that after 3.5 hours of crystallization, the synthesis of 13X zeolite is still in its initial stage. Accordingly, the obtained sample has a small specific surface area and very low adsorption capacity compared to all other experiments shown in this paper. The diffractogram of this sample, comparatively shown in Figure 8 with the diffractograms of other samples from this series,

Table 3. Results of the analysis of 13X zeolite powders synthesized at different durations of the crystallization reaction

Synthesis number	$\tau_{cr.}$ [*min*]	D50 [*μm*]	Si/Al ratio
3	330	3.40	1.135
5	210	3.78	1.180
6	270	3.18	1.140
7	390	3.56	1.130

clearly shows a high proportion of the amorphous phase. In addition, it should be noted that in the diffractogram there are no other crystalline forms except 13X zeolite.

Prolonging the synthesis by 1h, that is, after 4.5*h* of crystallization, resulted in a crystallinity of about 88%, which indicates that a large part of the conversion of the starting components into the crystalline phase of

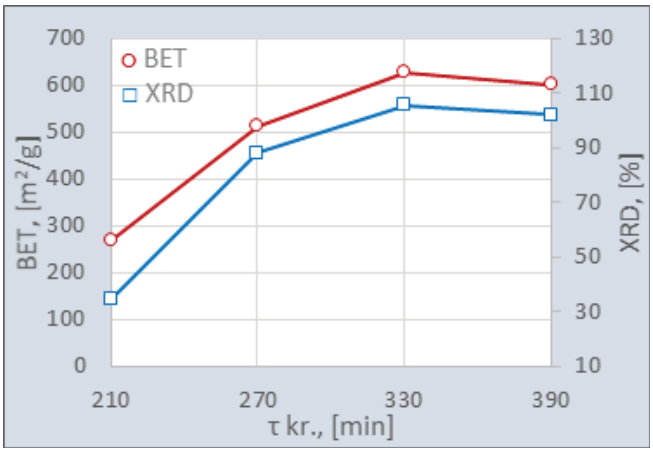

Figure 6. The trend of crystallinity values (□) and specific surface area (○) of the material in relation to the crystallization time

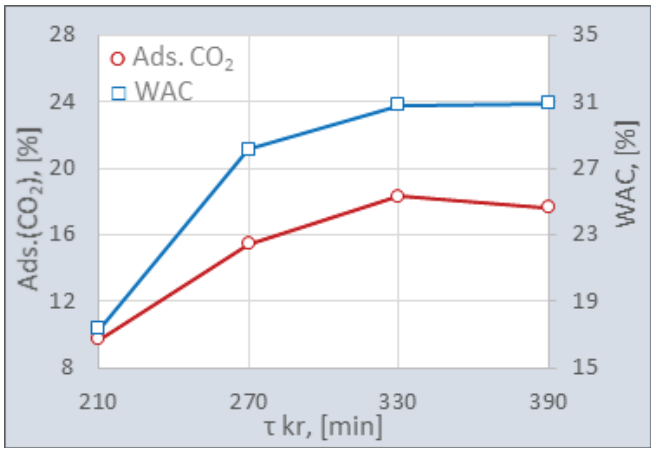

Figure 7. The trend of water adsorption (□) and carbon dioxide adsorption (○) values in relation to crystallization time

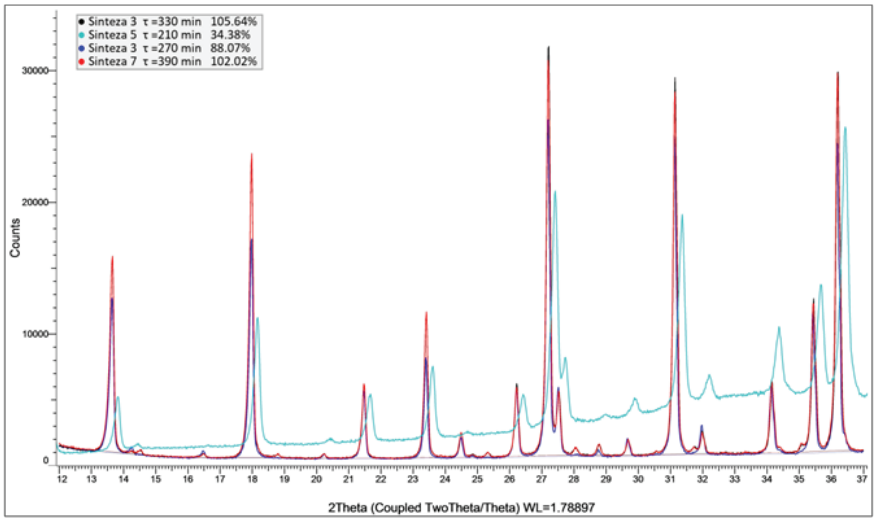

Figure 8. Diffractogram of the synthesis sample 3.5-7, performed at different crystallization time

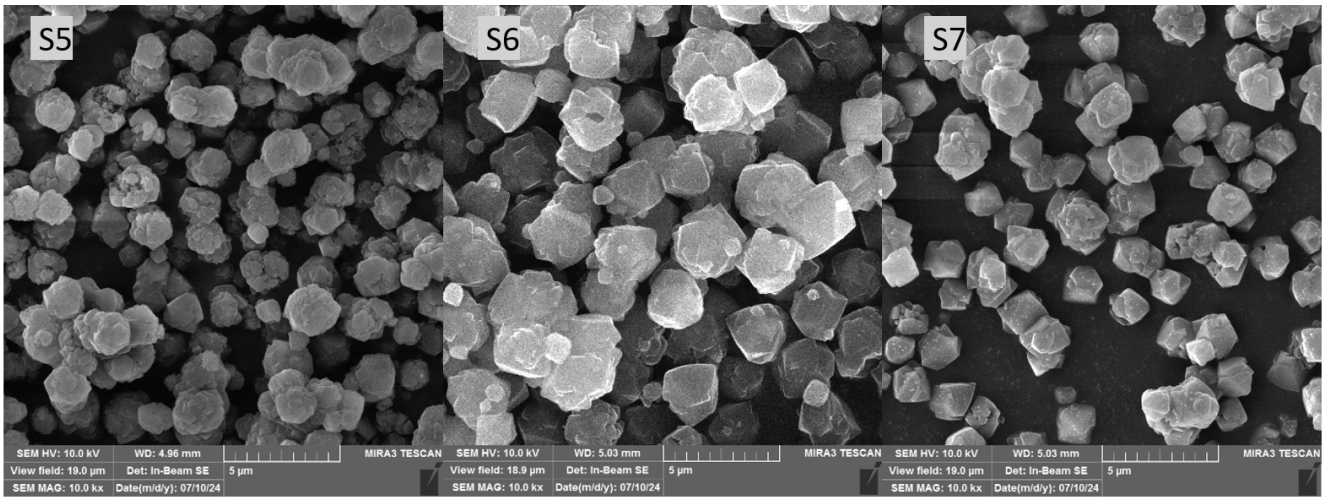

Figure 9. SEM images of samples from syntheses 5-7, performed at different durations of the crystallization reaction

13X zeolite takes place in this period. The results of other analyses of this sample follow its crystallinity, and this sample also shows respectable values of specific surface area (over 500 m^2/g) and adsorption capacities. However, as it turned out, to obtain a final product of high quality and adequate, satisfactory parameters, it is necessary to extend the crystallization time by another hour. The powder synthesized over 5.5 hours resulted in a 13X zeolite with a high crystallinity of over 100% with all other tested quality parameters of satisfactory values. Further extension of the synthesis (synthesis 7) did not contribute to higher crystallinity of the material, nor other quality parameters. On the contrary, in the case of the powder synthesized during 6.5 hours, there is even a noticeable drop in the values of the quality parameters.

It is noticeable on the diffractograms that all the samples, regardless of the time of crystallization, kept a high purity of the crystalline phase of 13X zeolite, which also corresponds to the observation from the previous part that the crystallization temperature of 90°C, applied in this series of syntheses, corresponds to the crystallization of 13X zeolite. The diffractogram of sample S7 synthesized during the longest period of crystallization (6.5*h*) is the only one showing traces of the presence of the second phase, and again the 4A crystal form.

This phenomenon may be the reason for slightly worse quality parameters in sample S7 compared to sample S3, which was synthesized under the same conditions during a shorter period of 1 hour. The appearance of the 4A (LTA) crystal form, as mentioned earlier, is not unusual in the synthesis of 13X zeolite, and traces of these crystals could have formed during the heating period and the very beginning of crystallization, where the parameters examined in this paper had no influence. It is also possible, however, that the time the suspension was kept in the reaction conditions was too long, and that, at the end of the crystallization of the 13X phase, the conditions favourable to the formation of other crystalline forms, including LTA zeolite, were obtained in the mother solution.

The SEM image of the sample from synthesis 5 (Fig. 9) shows particles without a clearly defined shape and crystal planes, mostly connected in agglomerates, which corresponds to the low crystallinity of this material and the high proportion of the amorphous phase. The development of crystallites from the amorphous hydrogel in this synthesis was interrupted due to insufficient synthesis time. Already in synthesis sample 6, synthesized 1h longer, the crystallites are better defined with more regular crystal planes (Fig. 9). Here, a significant proportion of smaller particles, below and around 1 µm, is noticeable, which are most likely formed by the breaking of agglomerates recorded in sample S5, and which later grow during further crystallization, and are not present to such an extent in samples synthesized during 5.5 and 6.5*h*. Due to this phenomenon, sample S6 has the lowest measured mean particle diameter in this series of samples (Tab. 3). Samples S3 (τ_{cr}.=5.5*h*; Fig. 5) and S7 (τ_{cr}.=6.5*h*; Fig.9) are again well-defined crystallites with a uniform morphology that corresponds to the results of other analyses. Additionally, on the particles of sample S7, very fine particle impurities are noticeable, which may be a consequence of the presence of the second phase observed by XRD analysis. The appearance of these small impurities on the surface of the crystallites indicates that their formation most likely occurred during the last hour of synthesis and that it is not desirable to maintain the suspension in reaction conditions for such a long time.

The three samples that have relevant crystallinity values, except sample S5, have an approximate Si/Al ratio that corresponds to the pure phase of 13X zeolite in these three samples. The crystallization of sample

S5 did not reach the final stage, so the Si/Al ratio in this sample is not a relevant parameter, although a slightly higher value indicates that in the first part of crystallization, the "wasting" of silicon species from the reaction system is more favoured than in the later stage of synthesis.

As expected, the best results of absorption of carbon dioxide and water are shown by the sample obtained by synthesis 3 (Fig. 7).

Effect of different Si/Al ratio

The Si/Al molar ratio in zeolite synthesis is observed through two cases - as the ratio of these components in the initial reaction mixture, that is, in the precursor, and as the ratio in the crystal structure. In the first case, it is a synthesis parameter that can have a decisive influence on the type and quality of the zeolite being synthesized. In the second case, it is an important characteristic of the obtained zeolite powder that affects properties such as hydrophobicity, thermal and chemical stability, activity of the crystal lattice, etc., so from that perspective, it can determine the quality of the synthesized powder. The silicate and aluminate species present in the initial reaction mixture, the precursor, react at different rates during crystallization, and partially, more or less, remain behind in the mother solution after crystallization, so that the Si/Al ratio of the precursor mainly affects the Si/Al ratio of the obtained powder, but these two parameters need not be monitored exclusively in parallel. Many zeolite species can only be synthesized within a certain range of the Si/Al ratio, which in the case of zeolites with a high aluminium content such as FAU and LTA zeolites is generally very narrow. Table 4 shows the results of analyses of zeolite 13X synthesized from precursors with different Si/Al ratios to show the influence of this parameter on the Si/Al ratio in the powder and other characteristics. Diagrams of basic dependencies are given in Fig. 10 and Fig.11.

According to the obtained results, zeolite 13X with a high degree of crystallinity was obtained at higher applied Si/Al ratios in the precursor, of 1.35 and 1.40. At these Si/Al ratios, the synthesized powders had higher crystallinity than the standard 13X zeolite sample. However, already with lowering the initial Si/Al ratio to 1.30, the crystallinity of the 13X phase decreased significantly, and an additional decrease in crystallinity was recorded with further lowering of the Si/Al ratio in the precursor.

Other qualitative properties that were determined in this case also follow the crystallinity trend, so we can say that with an increase in the Si/Al molar ratio in the range shown, the specific surface area of the material as well as water and CO_2 adsorption capacity

Table 4. Results of analysis of 13X zeolite powders synthesized with different Si/Al molar ratios of the initial reaction mixture

Synthesis number	Si/Al (prec.) [-]	D50 [μm]	Si/Al (powder) [-]
3	1.35	3.40	1.135
8	1.40	3.38	1.145
9	1.30	3.91	1.150
10	1.25	3.14	1.105

increases. It should be noted (Fig. 10 and Fig. 11) that the increase in the values of crystallinity, specific surface area and adsorption capacities between the samples synthesized at Si/Al 1.35 and 1.40 are very low, and that the values of these parameters in these two samples (synthesis 3 and 8) are very close, which indicates that in that range of Si/Al value of the precursor, the system reached the optimal value for obtaining 13X zeolite of high crystallinity and good quality.

The Si/Al ratio of the synthesized powders is significantly lower in synthesis samples 9 and 10, where this ratio was lower in the starting mixture, i.e. precursor, but the difference in values in the synthesized powder is even greater than the difference in values related to the precursor. The lower Si/Al ratio of the precursor therefore influenced this ratio to be lower in the obtained powders, and this phenomenon needs to be considered in more detail by looking at the diffractograms of the samples in Fig. 12.

The diffractograms of the samples from this series indicate a clear difference in the crystallinity and composition of the powders obtained at different Si/Al ratios in the precursor. The diffractograms of samples 3 and 8, synthesized from precursors with a higher Si/Al ratio, show well-defined peaks characteristic of 13X zeolite. These peaks are of high intensity, and next to them, no significant presence of other phases is observed, which corresponds to the high values of the results of the analyses shown in Table 1. On the other hand, when observing the diffractograms of samples from syntheses 9 and 10, it can be seen that in addition to the peaks of the 13X phase present peaks of 4A zeolite.

By reducing the molar ratio of Si/Al, the composition of the starting reaction mixture shifts towards the conditions corresponding to the formation of 4A zeolite crystals, which affected its appearance in the powders from syntheses 9 and 10. At the same time, sample 9 does not have the presence of an amorphous phase, which means that the reaction components completely crystallized, but with the appearance of a second crystalline phase. Due to

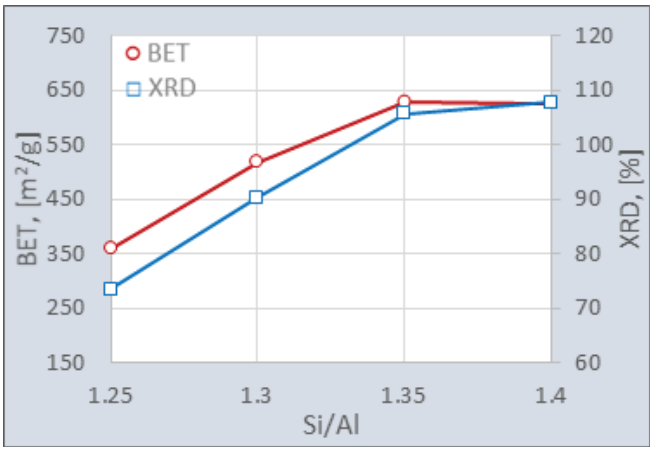

Figure 10. Trend of crystallinity values (□) and specific surface area (○) of the material in relation to the Si/Al molar ratio of the starting reaction mixture

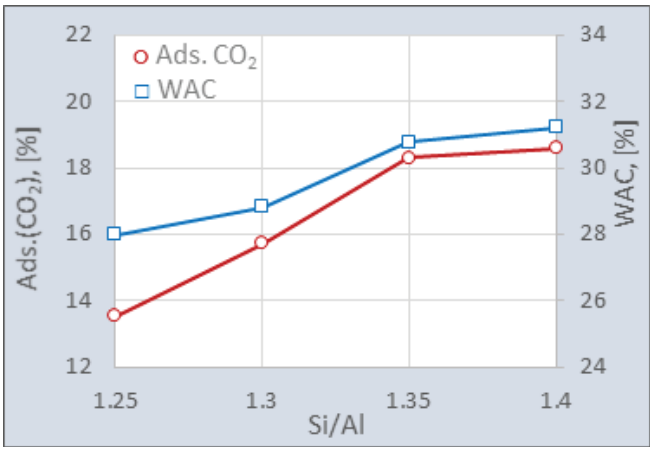

Figure 11.The trend of water adsorption (□) and carbon dioxide adsorption (○) values in relation to the Si/Al molar ratio of the starting reaction mixture

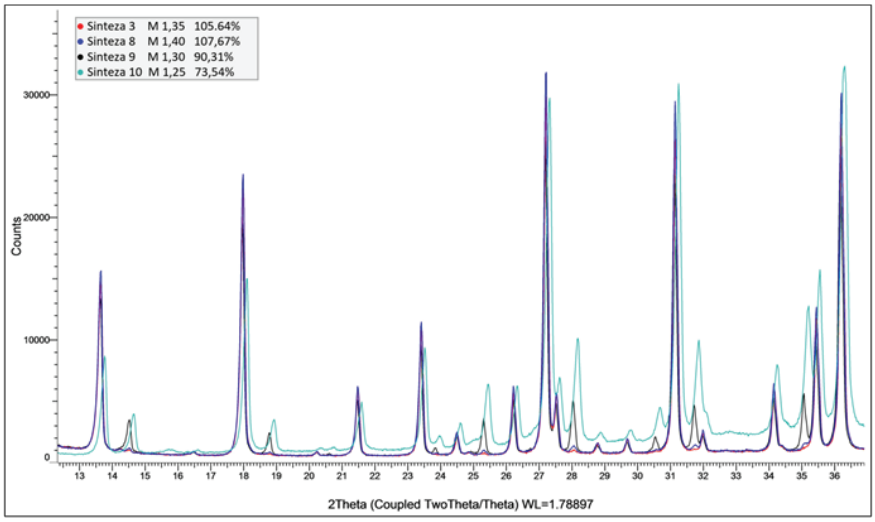

Figure 12. Diffractogram of a sample of syntheses 3, 8-10, performed with different Si/Al molar ratios of the starting reaction mixture

complete crystallization, the analysis results of this powder shown in the Table are not so drastically worse with a specific surface of over 500m²/g. The diffractogram of the sample with the lowest initial Si/Al molar ratio shows a significantly worse situation. In this case, in addition to the significant presence of the 4A crystalline form, there is also a high proportion of the amorphous phase, which caused the results of the analyses to be significantly different from the other samples from this series. The presence of an amorphous phase can be explained by the fact that the conditions of crystallization in this synthesis, i.e. primarily the Si/Al ratio, did not fully correspond to any of the crystal forms present.

The presence of the 4A crystalline phase in the powders of syntheses 9 and 10 probably influenced the observed decrease in the Si/Al ratio in these powders after crystallization, considering that this zeolite crystallizes with a lower Si/Al ratio in its composition than the 13X zeolite. This means that the reduction of the Si/Al ratio in the precursor did not affect the reduction of this value in the 13X zeolite crystals, but only the appearance of another crystalline form where this ratio is lower.

There are no unusual phenomena in the SEM images of synthesis samples 8 and 9, i.e., as in the case of sample 3 whose SEM was shown earlier, there are defined crystallites of uniform size and shape that correspond to highly crystalline materials. On the other hand, the SEM image of sample 10 shows a significant amount of impurities on the surface and between the usual crystalline particles, which we can assume are the remains of the previously mentioned amorphous phase. Given that the particles of this impurity are very small, they may be the reason for the slightly lower value of the mean diameter of the particles in sample 10 compared to other samples shown in this series and also in the paper. Apart from that, no dependence

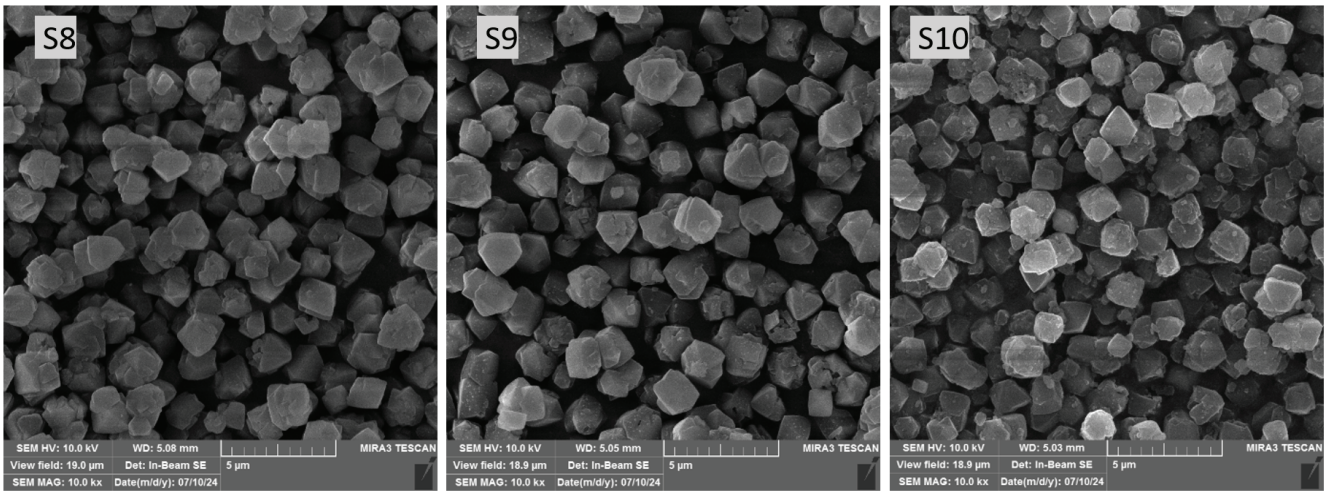

Figure 13. SEM images of samples from syntheses 8-10, performed with different Si/Al molar ratios of the starting reaction mixture

of the value of the mean diameter of the particles on the Si/Al ratio of the precursor is observed.

CONCLUSION

The synthesis of 13X zeolite, a material widely used in applications such as gas adsorption, catalysis, and ion exchange due to its high surface area and exceptional adsorption properties, was carefully studied with respect to three key parameters: crystallization temperature, crystallization time, and the Si/Al molar ratio. The results provide a detailed understanding of how each of these factors influences the quality and characteristics of the synthesized zeolite.

An increase in crystallization temperature from 82°C to 94°C led to a significant enhancement in the crystallinity of the 13X zeolite. Higher temperatures not only promoted the formation of a highly crystalline and pure 13X zeolite phase but also increased the material's specific surface area, contributing to its superior adsorption capacities. However, lower temperatures (82°C–86°C) favoured the formation of 4A zeolite as an impurity. This phase, while common in other applications, lowers the overall adsorption efficiency of the material, making it less suitable for applications where a high surface area of 13X is critical.

The crystallization time was found to be a crucial factor as well. A time of 5.5 hours was determined to be optimal for achieving high-quality 13X zeolite. Shorter crystallization times (e.g., 3.5 hours) resulted in materials with low crystallinity and poor adsorption properties, as the synthesis was still in its early stages. On the other hand, extending the crystallization time to 6.5 hours led to the appearance of 4A zeolite as a secondary phase, reducing the overall quality of the material.

The Si/Al molar ratio in the precursor also played a decisive role in the synthesis outcome. Higher ratios (1.35–1.40) yielded zeolite powders with superior crystallinity and adsorption properties, closely matching or even surpassing the characteristics of standard 13X zeolite. However, lowering the Si/Al ratio (to 1.30 or below) led to the appearance of 4A zeolite, reducing both crystallinity and adsorption performance. In the sample with the lowest Si/Al ratio (1.20), a significant presence of the amorphous phase further degraded the material's overall quality, resulting in lower surface area and inferior adsorption capacity.

In summary, the study identified optimal synthesis conditions for producing high-quality 13X zeolite: crystallization temperature of 94°C, time of 5.5 hours, and Si/Al molar ratio of 1.35–1.40. These conditions ensure the production of 13X zeolite with high crystallinity, large specific surface area, and excellent adsorption properties, making it highly suitable for industrial applications. Deviations from these parameters—such as lower temperatures, shorter crystallization times, or lower Si/Al ratios—resulted in impurities like 4A zeolite and amorphous phases, which compromise the material's quality. Given the importance of 13X zeolite in various fields, understanding and optimizing these synthesis parameters is essential for producing a material that meets the high standards required for its diverse applications.

Acknowledgements: *Certain aspects of the research, analytical and chemical analysis of the sorption characteristics are one of the points of interest in the research activities of the EURO-TITAN project.*

REFERENCES

Alshahidy, B. A., & Abbas, A. S. (2021). Comparative study on the catalytic performance of a 13X zeolite and its dealuminated derivative for biodiesel production. *Bulletin of Chemical Reaction Engineering and Catalysis*, *16*(4), 763–772. https://doi.org/10.9767/BCREC.16.4.11436.763-772

Al-Shawabkeh, A. F., Al-Najdawi, N., & Olimat, A. N. (2023). High-purity oxygen production by pressure vacuum swing adsorption using natural zeolite. *Results in Engineering*, *18*, 101119. https://doi.org/10.1016/J.RINENG.2023.101119

Anbia, M., Mohammadi Nejati, F., Jahangiri, M., Eskandari, A., & Garshasbi, V. G. (2015). Optimization of Synthesis Procedure for NaX Zeolite by Taguchi Experimental Design and its Application in CO2 Adsorption. *Journal of Sciences, Islamic Republic of Iran*, *26*(3), 213–222. https://jsciences.ut.ac.ir/article_55309.html

Auerbach, S. M., Carrado, K. A., & Dutta, P. K. (2003). Handbook of Zeolite Science and Technology. *Handbook of Zeolite Science and Technology*. https://doi.org/10.1201/9780203911167/HANDBOOK-ZEOLITE-SCIENCE-TECHNOLOGY-SCOTT-AUERBACH-KATHLEEN-CARRADO-PRABIR-DUTTA

Bareschino, P., Mancusi, E., Forgione, A., & Pepe, F. (2020). Biogas purification on Na-X Zeolite: Experimental and numerical results. *Chemical Engineering Science*, *223*, 115744. https://www.academia.edu/94631624/Biogas_purification_on_Na_X_Zeolite_Experimental_and_numerical_results,

P., Delgado, J. A., Águeda, V. I., Gutiérrez, P., & Uguina, M. A. (2019). Multicomponent adsorption of H2, CH4, CO and CO2 in zeolites NaX, CaX and MgX. Evaluation of performance in PSA cycles for hydrogen purification. *Microporous and Mesoporous Materials*, *286*, 187–198. https://doi.org/10.1016/J.MICROMESO.2019.05.021

Chen, S., Zhu, M., Tang, Y., Fu, Y., Li, W., & Xiao, B. (2018). Molecular simulation and experimental investigation of CO2 capture in a polymetallic cation-exchanged 13X zeolite. *Journal of Materials Chemistry A*, *6*(40), 19570–19583. https://doi.org/10.1039/C8TA05647A

Cmarik, G. E., & Knox, J. C. (2018). *Co-Adsorption of Carbon Dioxide on Zeolite 13X in the Presence of Preloaded Water*. 48th International Conference on Environmental Systems. http://hdl.handle.net/2346/74024

Collins, F., Rozhkovskaya, A., Outram, J. G., & Millar, G. J. (2020). A critical review of waste resources, synthesis, and applications for Zeolite LTA. *Microporous and Mesoporous Materials*, *291*. https://doi.org/10.1016/J.MICROMESO.2019.109667

Database of Zeolite Structures. (n.d.). Retrieved September 11, 2024, from https://www.iza-structure.org/databases/

Esfandian, H., & Garshasbi, V. (2020). Investigation of methane adsorption on molecular sieve zeolite (from natural materials). *Gas Processing Journal*, *8*(2), 35–50. https://doi.org/10.22108/GPJ.2020.121907.1080

Garshasbi, V., Jahangiri, M., & Anbia, M. (2017). Equilibrium CO 2 adsorption on zeolite 13X prepared from natural clays. *Applied Surface Science*, *393*, 225–233. https://doi.org/10.1016/J.APSUSC.2016.09.161

Gholipour, F., & Mofarahi, M. (2009). Adsorption equilibrium of methane and carbon dioxide on zeolite 13X: Experimental and thermodynamic momodelling*Journal of Supercritical Fluids*, *111*, 47–54. https://doi.org/10.1016/J.SUPFLU.2016.01.008

Houchins, G., Pande, V., Khetan, A., -, al, Norouzi, N., Akhtar Choudhury, F., El-Kaderi, H. M., Sameer, S., & Eswaran, P. (2020). Development and integration of oxygen generator for home air conditioner. *IOP Conference Series: Materials Science and Engineering*, *912*(4), 042054. https://doi.org/10.1088/1757-899X/912/4/042054

Janković, M. B., Perušić, M. D., Damjanović, V. M., Filipović, R. L., Obrenović, Z. B., Tadić, G. S., & Kostić, D. D. (2023). Influence of suspension heating rate on properties of zeolite 13X. *HEMIJSKA INDUSTRIJA (Chemical Industry)*, *77*(4), 275–282. https://doi.org/10.2298/HEMIND230418023J

Liu, J., Sun, X., Li, N., Tan, T., Zhang, F., Sun, M., & Liu, Q. (2024). Effect of synthesis conditions on the properties of 13X zeolites for CO2 adsorption. Environmental Pollutants and Bioavailability, 36(1). https://doi.org/10.1080/26395940.2024.2387683

Liu, L., Singh, R., Li, G., Xiao, G., Webley, P. A., & Zhai, Y. (2012). Synthesis of hydrophobic zeolite X@ SiO2core-shelll composites. *Materials Chemistry and Physics*, *133*(2–3), 1144–1151. https://doi.org/10.1016/J.MATCHEMPHYS.2012.02.028

Liu, L. Y., Du, T., Fang, X., Che, S., & Wang, X. G. (2014). Preparation of hydrophobic zeolite 13X@ SiO2 and their adsorption properties of CO2 and H2O. *Advanced Materials Research*, *1053*, 311–316. https://doi.org/10.4028/WWW.SCIENTIFIC.NET/AMR.1053.311

Mofarahi, M., & Shokroo, E. J. (2013). *COMPARISON OF TWO PRESSURE SWING ADSORPTION PROCESSES FOR AIR SEPARATION USING ZEOLITE 5A AND ZEOLITE 13X*.

Morales-Ospino, R., Santiago, R. G., Siqueira, R. M., de Azevedo, D. C. S., & Bastos-Neto, M. (2020).

Assessment of CO_2 desorption from 13X zeolite for a prospective TSA process. *Adsorption*, *26*(5), 813–824. https://doi.org/10.1007/S10450-019-00192-5

Price, L., Leung, K. M., & Sartbaeva, A. (2017). Local and Average Structural Changes in Zeolite A upon Ion Exchange. *Magnetochemistry 2017, Vol. 3, Page 42*, *3*(4), 42. https://doi.org/10.3390/MAGNETOCHEMISTRY3040042

Shirani, B., Kaghazchi, T., & Beheshti, M. (2010). Water and mercaptan adsorption on 13X zeolite in natural gas purification process. *Korean Journal of Chemical Engineering*, *27*(1), 253–260. https://doi.org/10.1007/S11814-009-0327-Z

Sigot, L., Fontseré Obis, M., Benbelkacem, H., Germain, P., & Ducom, G. (2016). Comparing the performance of a 13X zeolite and an impregnated activated carbon for H 2 S removal from biogas to fuel an SOFC: Influence of water. *International Journal of Hydrogen Energy*, *41*(41), 18533–18541. https://doi.org/10.1016/J.IJHYDENE.2016.08.100

Tahraoui, Z., Nouali, H., Marichal, C., Forler, P., Klein, J., & Daou, T. J. (2020). Influence of the Compensating Cation Nature on the Water Adsorption Properties of Zeolites. *Molecules 2020, Vol. 25, Page 944*, *25*(4), 944. https://doi.org/10.3390/MOLECULES25040944

Yahya, M. M., & Hussein, H. Q. (2019). Adsorption Desulfurization Of Iraqi Heavy Naphtha Using Zeolite 13x. *Association of Arab Universities Journal of Engineering Sciences*, *26*(2), 12–18. https://doi.org/10.33261/JAARU.2019.26.2.003

Zafanelli, L. F. A. S., Henrique, A., Aly, E., Silva, J. A. C., & Rodrigues, A. E. (2024). Purification of green hydrogen from natural gas grids using zeolite 13X. *WASTES: Solutions, Treatments and Opportunities IV - Selected Papers from the 6th International Conference Wastes*, *2023*, 63–68. https://doi.org/10.1201/9781003345084-11/PURIFICATION-GREEN-HYDROGEN-NATURAL-GAS-GRIDS-USING-ZEOLITE-13X-ZAFANELLI-HENRIQUE-ALY-SILVA-RODRIGUEa